

Vibrational Dynamics and Heat Capacity of Poly(p-phenylene)



Physics

KEYWORDS: Vibrational dynamics, Density-of-state, Heat capacity, IR spectra

Irfan Ahmad Khan

Department of Physics, Integral University, Lucknow-226026, India

Irfan Ali Khan

Department of Physics, Integral University, Lucknow-226026, India

ABSTRACT

Using Urey-Bradley force field and Wilson's GF matrix method as modified by Higgs, normal modes of vibration and their dispersions in poly(p-phenylene) (PPP) have been obtained. It provides a detailed interpretation of IR spectra. Characteristic feature of dispersion curves such as regions of high density-of-states, repulsion and character mixing of dispersion modes are discussed. Predictive values of heat capacity as a function of temperature are also reported.

1. Introduction

Most of the commercially produced organic polymers are electrical insulators. Conducting polymers, which are mostly organic, have delocalized bonds that create a band gap like any conductor. When the material is doped its electrical conductivity enhanced. Almost all known conducting polymers are semiconductors due to the band structure and low electronic mobility. However, so-called zero band gap conducting polymers may behave like metals. Among different conducting polymers, poly(p-phenylene) (PPP) (Fig. 1) is an interesting polymer, used in organic light emitting devices, biosensors, solar energy cells, laser materials, electrochemical actuators etc.¹⁻⁴ due to its high conductivity^{3,5}.

Fig.1: Chemical repeat unit of PPP



From *ab-initio* calculations Bredas et al. have found the variation of torsion angle from 37.8° to 2°. Further, they have reported the torsion angle between two consecutive rings is 2° which support the planar geometry of PPP⁶. Chemically PPP was synthesized by oxidative polymerization of benzene^{7,8} and doped with FeCl₃⁹. Electrical conductivity response of doped PPP (dPPP) towards CO, H₂ and NH₃ was investigated and disclosed that the electrical conductivity sensitivity of dPPP increases with increasing NH₃ concentration¹⁰. Vibrational spectroscopy provides useful information concerning the conformation of conducting polymers. It is a very important tool for probing into conformation through conformational sensitive modes. Theoretically, the vibrational dynamics of various conducting polymers have been studied by normal mode analysis¹¹⁻¹⁴. Navarrete *et al.* have interpreted the infrared and Raman spectra of PPP in the pristine and doped states using the Effective Conjugation Coordinate theory^{15,16}. They have also reported dispersion curves of PPP. However, they did not take their study to a logical end by evaluating thermodynamic parameters such as heat capacity. Further, the MNDO calculated scaled force constants used by these authors took into account only limited interactions. They ignored some of the important interactions, like torsional and non-bonded interactions. Hence, the need arises for redoing this problem to arrive at a logical end.

In general the IR absorption, Raman spectra, and inelastic neutron scattering from polymeric systems are very complex and cannot be unraveled without the full knowledge of their dispersion curves. Dispersion curves and dispersion profiles also provide information about the extent of coupling along the polymeric chain or between the chains. The frequency of a given mode depends upon the sequence length of ordered conformation. Thus, the study of phonon dispersion in polymeric systems continues to be of topical importance. In the present work, we report a complete normal mode analysis of PPP using the Urey-

Bradley force field, including calculation of the phonon dispersion and heat capacity obtained via the density-of-states derived from the dispersion curves. The experimental data of IR reported by previous authors¹⁵⁻¹⁷ used for comparison. The calculated value of heat capacity is in fairly good agreement with experimental data¹⁸.

2. Theoretical Approach

2.1 Normal Modes Calculation

The calculation of normal modes frequencies has been carried out according to the well-known Wilson's GF¹⁹ matrix method as modified by Higgs²⁰ for an infinite polymeric chain. It consists of writing the inverse kinetic energy matrix G and the potential energy matrix F in terms of internal coordinates. In the case of an infinite isolated helical polymer, there are infinite number internal coordinates that lead to G and F matrices of infinite order. Due to the screw symmetry of the polymer, a transformation similar to that given by Born and Von Karman can be performed that reduces the infinite problem to finite dimensions²¹. The vibrational secular equation, which gives normal modes frequencies and their dispersion as a function of phase angle, has the form:

$$| G(\delta) F(\delta) - \lambda(\delta) | = 0, \quad 0 \leq \delta \leq \pi \quad \dots\dots\dots 1$$

The vibrational frequencies $\nu(\delta)$ (in cm⁻¹) are related to the Eigen values $\lambda(\delta)$ by the following relation:

$$\lambda(\delta) = 4\pi^2 c^2 \nu^2(\delta) \quad \dots\dots\dots 2$$

A plot of $\nu_i(\delta)$ versus δ gives the dispersion curve for the *i*th mode.

2.2 Calculation of Heat Capacity

Dispersion curves can be used to calculate the specific heat of a polymeric system. For a one dimensional system the density-of-states function or the frequency distribution function expresses the way energy is distributed among the various branches of normal modes in the crystal, is calculated from the relation

$$g(\nu) = \sum_{j(\delta)=nj} (\partial n_j / \partial \delta)^{-1} \quad \dots\dots\dots 3$$

The sum is over all the branches *j*. considering a solid as an assembly of harmonic oscillators, the frequency distribution *g* (ν) is equivalent to a partition function. The constant volume heat capacity can be calculated using Debye's relation

$$C_v = \sum g(\nu_j) K N_A (\hbar \nu_j / K T)^2 [\exp(\hbar \nu_j / K T) / \{\exp(\hbar \nu_j / K T) - 1\}]^2 \quad \dots\dots 4$$

The constant volume heat capacity *C_v*, given by above equation, can be converted into constant-pressure heat capacity *C_p* using the Nernst-Lindemann approximation^{22,23};

$$C_p - C_v = 3 R A_0 (C_p^2 T / C_v T_m^0) \quad \dots\dots\dots 5$$

Where A_0 is a constant often of a universal value [$3.9 \times 10^{-3}(\text{K mol})/J$] and T_m^0 is the equilibrium melting temperature.

3. Results and Discussion

The structure of PPP has been determined by using the molecular modeling technique, with the help of CS-Chemdraw. There are 11 atoms per residue unit, hence, there would be $11 \times 3 - 4 = 29$ normal modes of vibration. The vibrational frequency have been calculated for δ values ranging from 0 to π in intervals of 0.05π . The optically calculated active modes are matched with the frequencies obtained from the IR spectra. The Urey-Bradley force constants were initially transferred from the earlier work on molecules having similar groups and were further refined by using the least-square method as describe earlier²⁴. The four zero frequencies at $\delta = 0$ correspond to acoustic modes, three representing translations along the three axis and the fourth one is rotation around the chain axis. All vibrational modes along their PEDs' are given in Table 1 and 2 at $\delta = 0.0$ and $\delta = 1.0$, respectively.

Table 1: Vibrational modes of PPP at $\delta = 0.0$
Frequency (cm^{-1})

Calculated	Observed	% PED (Potential Energy Distribution) at $\delta = 0$
3108	3100	v(C-H)(99)
3062	3060	v(C-H)(99)
3061	3060	v(C-H)(99)
3059	3060	v(C-H)(100)
1658	1660	v(C=C)(68)+v(C-C)(24)+ ϕ (C-C-H)(5)
1616	1620	v(C=C)(72)+v(C-C)(18)+ ϕ (C-C-H)(9)
1611	1609	v(C=C)(77)+ ϕ (C-C-H)(8)+v(C-C)(8)+ ϕ (C-C-C)(7)
1255	1260	ϕ (C-C-H)(55)+v(C-C)(40)
1222	1220	v(C-C)(68)+v(C=C)(16)+ ϕ (C-C-H)(11)
1158	1170	v(C-C)(59)+ ϕ (C-C-H)(36)
1111	1110	ϕ (C-C-H)(93)
1001	1000	ϕ (C-C-H)(92)+v(C=C)(8)
933	940	ϕ (C-C-H)(53)+v(C-C)(41)
881	880	ϕ (C-C-H)(42)+v(C-C)(41)+v(C=C)(13)
679	684	v(C-C)(49)+ ϕ (C-C-C)(32)+v(C=C)(12)+ ϕ (C-C-H)(7)
673	660	ϕ (C-C-C)(64)+ ϕ (C-C-H)(18)+v(C-C)(14)
577	578	ω (C-H)(90)+ τ (C=C)(6)
563	550	ω (C-H)(95)
492	510	ω (C-H)(83)+ τ (C=C)(10)+ τ (C-C)(6)
469	464	ω (C-H)(90)+ τ (C=C)(9)
416	420	ϕ (C-C-C)(63)+ ϕ (C-C-H)(34)
340		ϕ (C-C-C)(89)
163		ϕ (C-C-C)(43)+ τ (C=C)(32)+ τ (C-C)(19)
93		τ (C-C)(34)+ ϕ (C-C-C)(30)+ τ (C=C)(30)+ ω (C-H)(5)
81		τ (C=C)(61)+ τ (C-C)(27)+ ω (C-H)(9)
73		τ (C=C)(87)+ ω (C-H)(13)
4		τ (C-C)(51)+ ϕ (C-C-C)(30)+ τ (C=C)(14)
2		ϕ (C-C-C)(38)+ τ (C-C)(27)+ τ (C=C)(22)+ ϕ (C-C-H)(7)
.229		ϕ (C-C-C)(68)+ ϕ (C-C-H)(28)
.174		ϕ (C-C-H)(76)+ ϕ (C-C-C)(20)

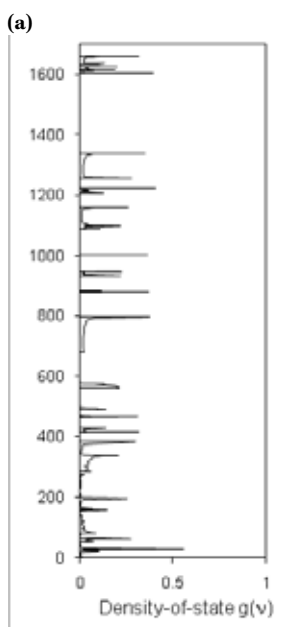
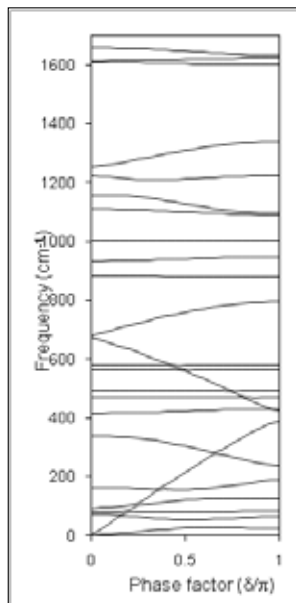
Table 2: Vibrational modes of PPP at $\delta = 1.00$
Frequency (cm^{-1})

Calculated	Observed	% PED (Potential Energy Distribution) at $\delta = 1.00$
3108	3100	v(C-H)(99)
3062	3060	v(C-H)(99)
3061		v(C-H)(99)
3059		v(C-H)(100)
1631	1620	v(C=C)(74)+v(C-C)(14)+ ϕ (C-C-H)(9)
1626		v(C=C)(72)+v(C-C)(22)
1602	1600	v(C=C)(75)+ ϕ (C-C-H)(12)+v(C-C)(9)
1340	1320	v(C-C)(71)+ ϕ (C-C-H)(22)+ ϕ (C-C-C)(5)
1225	1200	v(C-C)(48)+ ϕ (C-C-H)(37)+ ϕ (C-C-C)(11)
1097	1100	ϕ (C-C-H)(80)+v(C-C)(14)
1089		ϕ (C-C-H)(74)+v(C-C)(21)
1002	1000	ϕ (C-C-H)(91)+v(C=C)(9)
948	940	ϕ (C-C-H)(63)+v(C-C)(29)
880	880	v(C-C)(79)+v(C=C)(20)
795	800	v(C-C)(39)+ ϕ (C-C-H)(26)+ ϕ (C-C-C)(26)+v(C=C)(10)
577	578	ω (C-H)(90)+ τ (C=C)(6)
563	550	ω (C-H)(95)
492	510	ω (C-H)(83)+ τ (C=C)(10)+ τ (C-C)(6)
469	464	ω (C-H)(89)+ τ (C=C)(9)
431	440	ϕ (C-C-C)(65)+ ϕ (C-C-H)(30)
424	420	ϕ (C-C-C)(85)+ ϕ (C-C-H)(11)
388	400	ϕ (C-C-C)(48)+v(C-C)(35)+ ϕ (C-C-H)(12)
239	230	ϕ (C-C-C)(81)+v(C-C)(10)
189		ϕ (C-C-C)(86)+ τ (C=C)(6)
125		τ (C=C)(59)+ τ (C-C)(27)+ ω (C-H)(11)
83		τ (C=C)(55)+ τ (C-C)(34)+ ω (C-H)(7)
65		τ (C=C)(79)+ ω (C-H)(12)+ ϕ (C-C-C)(6)
24		τ (C-C)(73)+ τ (C=C)(22)
2		ϕ (C-C-H)(27)+ τ (C-C)(23)+ τ (C=C)(23)+ ϕ (C-C-C)(23)
.302		ϕ (C-C-C)(50)+ ϕ (C-C-H)(48)

3.1 Dispersion Curves

The dispersion curves below the 1700 cm^{-1} are shown in Fig. 2a. The modes above the 1700 cm^{-1} are either non dispersive or their dispersion is less than 5 cm^{-1} .

Convergence of various modes is the interesting feature of dispersion curves, i.e., the modes that are separated by a large wave number at the zone center, are comes very close at the zone boundary. This convergence arises mainly because of the close sharing of potential energy in different measures by the various modes. For example, the two zone centered modes calculated at 1158 and 1110 cm^{-1} show



(b)
Fig. 2: Dispersion curves (a) Density-of-state (b) of PPP (0–1700 cm⁻¹)

convergence, the modes 1158 and 1110 cm⁻¹ attract each other with the change of δ value and it can be observed that they are separated by 48 wave numbers at the zone center while at the zone boundary they are separated by 8 wave numbers.

Another interesting feature of dispersion curves is exchange of character which occurs at repulsion point. The modes calculated at 340 and 163 cm⁻¹ show repulsion at $\delta = 0.70$. These two modes are separated by 177 wave numbers at $\delta = 0.0$, but at $\delta = 0.70$, they are separated by only 20 wave numbers, and at $\delta = 1.00$ they are separated by 149 wave numbers.

3.2 Heat Capacity

The dispersion curves obtained for PPP have been used to calculate the density-of-state and heat capacity as a function of temperature. The density-of-state is shown in Fig. 2b. Variation of heat capacity as a function of temperature of PPP is shown in Fig. 3.

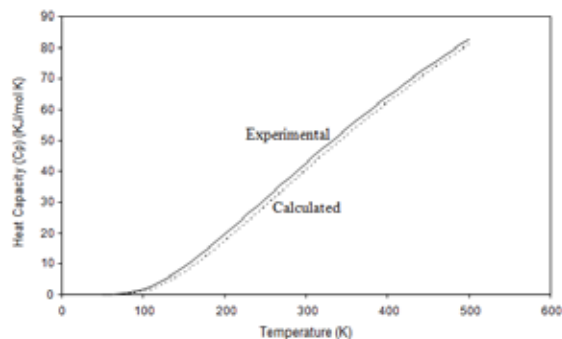


Fig.3: Variation of heat capacity with temperature of PPP

4. Conclusions

The vibrational dynamics of PPP can be satisfactorily interpreted from the dispersion curves and dispersion profile of the normal modes of PPP as obtained by Higg's method for infinite systems. Some of the internal symmetry dependent features such as attraction and exchange of character are also well understood.

REFERENCE

- [1] G. Grem, V. Martin, F. Meghdadi, C. Paar, J. Stampfl, J. Sturm, S. Tasch, G. | Leising, *Syn. Met.* 71 (1–3) (1995) 2193–2194. | [2] K. Arshak, V. Velusamy, O. Korostynska, K. O. Stasiak, C. Adley, *IEEE | Sensors J.* 9 (12) (2009) 1942–1951. | [3] K. Gurunathan, A.V. Murugan, R. Marimuthu, U.P. Mulik, D.P. Amalnerkar, | *Mater. Chem. Phys.* 61 (1999) 173–191. | [4] A.K. Bakhshi, G. Bhalla, J. Sci. Ind. Res.63 (2004) 715–728. | [5] D.M. Ivory; G.G. Miller; J.M. Sowa; L.W. Shacklette; R.R. Chance; R.H. | Baughman *J. Chem. Phys.* 71(3) (1979) 1506–1507. | [6] J.L. Bredas, B. Themans, J.M. Andre, *Phys. Rev. B* 26 (10) (1982) 6000– | 6002. | [7] P. Kovacic, A. Kyriakis, *J. Am. Chem. Soc.* 85 (1963) 454–458. | [8] P. Kovacic, J. Oziomek, *J. Org. Chem.* 29 (1964)100–104. | [9] T. Shiga, A. Okada, T. Kurauchi, *Macromolecules* 26 (1993) 6958–6963. | [10] P. Phumman, S. Niamlang, A. Sirivat, *Sensors* 9 (2009) 8031–8046. | [11] A.K. Mishra, P. Tandon, *J. Phys. Chem. B* 113 (29) (2009) 9702–9707. | [12] P. Ali, S.I. Ansari, S. Srivastava, V.D. Gupta, *Spectrochim. Acta A* 93 (2012) | 149–154. | [13] P. Ali, S. Srivastava, S.I. Ansari, V.D. Gupta, *Spectrochim. Acta A* 111 | (2013) 86–90. | [14] P. Ali, M. Ahmad, S. Srivastava, V.D. Gupta, *J. Macromol. Sci. Part B:Phys.* 53:7 (2014) 1305–1317. | [15] J. Soto, V. Hernandez, J.T. Lopez Navarrete, *Synthetic Metal*, 51(1992) 229– | 238. | [16] V. Hernandez, J. Soto, J.T. Lopez Navarrete, *Synthetic Metal*, 57 (2–3) | (1993) 4461–4466. | [17] S. Li, Z. Li, Xi. Fang, G. Chen, Y. Huang, K. Xu, *J. App. Polym. Sci.*110, | (2008) 2085–2093. | [18] M.V. Nair, B. Wunderlich, *J. Phys. Chem. Ref. Data* 20 (2) (1991), 396. | [19] E.B. Wilson, J.C. Decuis, P.C. Cross, and *Molecular Vibrations: The | theory of infrared and Raman vibrational spectra*, Dover Publication, New York 1980. | [20] P.W. Higgs, *Proc. Roy. Soc. London* 220 (1953) 472 - 480. | [21] P. Tandon, V.D. Gupta, O. Prasad, S. Rastogi, V.P. Gupta, *J. Polym. Sci. B Polym. Phys.* 35 (1997) 2281–2292. | [22] R. Pan, M.N. Verma, B. Wunderlich, *J. Therm. Anal.* 35(1989) 955–961. | [23] K.A. Roles, A. Xenopoulos, B. Wunderlich, *Biopolymers* 33 (1993) 753–755. | [24] S. Srivastava, S. Srivastava, S.J. Laverne, P. Ali, V.D. Gupta, *J. App. Polym. Sci.* 122 (2011) 1376–138. |